

# Synthesis, Characterization, and Property Study of Coordination Polymers Constructed from Cd Salt and Mixed Ligands<sup>1</sup>

P. Zhang\*, J. Tong, and C. Y. Xing

College of Chemistry, Liaoning University, Shenyang, 110036 P.R. China

\*e-mail: zhangpeng@lnu.edu.cn

Received June 9, 2014

**Abstract**—Two interesting new coordination polymers  $\{[\text{Cd}(\text{Dcbpyno})(1,4'\text{-Bix})_{1.5}] \cdot 2\text{H}_2\text{O}\}_n$  (**I**) and  $[\text{Cd}(1,2'\text{-Cy})(4,4'\text{-Bipy})]_n$  (**II**) ( $\text{Dcbpyno} = 2,2\text{-bipyridine-3,3-dicarboxylate-1,1'-dioxide}$ ,  $1,4'\text{-Bix} = 1,4\text{-bis(imidazol-1-ylmethyl)benzene}$ ,  $1,2'\text{-Cy} = 4\text{-cyclohexene-1,2-dicarboxylate}$  and  $4,4'\text{-Bipy} = 4,4'\text{-bipyridine}$ ) have been synthesized under different conditions. The X-ray crystal structures of these two complexes are presented (CIF files CCDC nos. 905357 (**I**), 874125 (**II**)). Complex **I** exhibits three-dimensional network, while complex **II** shows an interesting two-dimensional covalent layer structure. Furthermore, the photocatalytic property of complex **I** and the fluorescent property of complex **II** were reported.

**DOI:** 10.1134/S107032841501011X

## INTRODUCTION

During the past decades, coordination polymers have attracted considerable attention because of their interesting topologies and crystal packing modes, alongside potential applications in many areas including gas storage, catalysis, magnetism, optics, as well as conductivity [1–6]. The rational design and controllable preparation of coordination polymers are highly influenced by the coordination geometry of the central atom, the structure of the organic ligand and the reaction conditions [7–9]. Among above factors, the nature of the organic ligand plays crucial role in manipulating the network structure of the coordination polymers [10–15]. It is well known that the carboxylate ligand plays an important role in coordination chemistry, which can adopt various coordination modes and link metal ions with different manners [16–20]. In the large family of carboxylates, 2,2-bipyridine-3,3-dicarboxylate-1,1'-dioxide (Dcbpyno) and 4-cyclohexene-1,2-dicarboxylate (1,2'-Cy) are an good organic ligands in constructing coordination polymers, because they possesses two carboxylate groups, which can be completely or partially deprotonated and may serve as potential anion groups [21].

Nowadays, studies reveal that coordination polymers built from mixed ligands of carboxylate groups and pyridyl groups not only are more adjustable through changing one of the above two organic ligands but also incorporate interesting properties of different functional groups [22–24]. Although many coordination polymers have been synthesized from Dcbpyno and 1,2'-Cy ligands, the complexes constructed from

Dcbpyno, 1,2'-Cy and nitrogen-containing ligands are still largely unexplored [25]. We can conclude that the coordination polymers constructed from these two kinds of ligands may exhibit interesting structural and physical properties.

Based on these points, to synthesize new coordination polymers based on Dcbpyno, 1,2'-Cy and nitrogen-containing ligands as well as enrich their coordination chemistry, herein, we reported the preparation and the crystal structure of two new coordination polymers:  $\{[\text{Cd}(\text{Dcbpyno})(1,4'\text{-Bix})_{1.5}] \cdot 2\text{H}_2\text{O}\}_n$  (**I**) and  $[\text{Cd}(1,2'\text{-Cy})(4,4'\text{-Bipy})]_n$  (**II**) ( $1,4'\text{-Bix} = 1,4\text{-bis(imidazol-1-ylmethyl)benzene}$ , and  $4,4'\text{-Bipy} = 4,4'\text{-bipyridine}$ ). Furthermore, the photocatalytic property of complex **I** and the fluorescent property of complex **II** were reported.

## EXPERIMENTAL

**Materials and methods.** All purchased chemicals were reagent grade and used without further purification. Elemental analyses (C, H, and N) were performed on a PerkinElmer 2400 CHN elemental analyzer. FT/IR spectra were recorded in the range 4000–400  $\text{cm}^{-1}$  on an Alpha Centaur FTIR spectrophotometer using a KBr pellet. TG analyses were performed on Perkin-Elmer TGA7 instrument in flowing  $\text{N}_2$  with a heating rate of  $10^\circ\text{C min}^{-1}$ . The UV-visible adsorption spectrum was recorded using a Hitachi U-3010 UV-visible spectrometer. Photoluminescence spectrum was measuring using a FL-2T2 instrument (SPEX, United States) with 450-W xenon lamp monochromatized by double grating (1200 gr/mu).

<sup>1</sup> The article is published in the original.

**Synthesis of I.** The mixture of  $\text{Cd}(\text{OAc})_2 \cdot 2\text{H}_2\text{O}$  (0.134 g, 0.5 mmol), Dcbpyno (0.138 g, 0.5 mmol), 1,4'-Bix (0.119 g, 0.5 mmol), and 8 mL  $\text{H}_2\text{O}$  was stirred for 30 min, and then the pH value was adjusted to 7 with 1 M NaOH. After stirring for another 15 min, the mixture was transferred to a 25 mL Teflon-lined stainless steel bomb and kept at 130°C under autogenously pressure for 4 days. The reaction system was cooled to room temperature during 24 h. A large amount of colorless crystals of **I** were obtained. The yield was 73% (based on Cd).

For  $\text{C}_{33}\text{H}_{31}\text{N}_8\text{O}_8\text{Cd}$

anal. calcd., %: C, 50.81; H, 4.01; N, 14.36.

Found, %: C, 50.67; H, 4.08; N, 14.25.

**Synthesis of II.** The mixture of  $\text{Cd}(\text{OAc})_2 \cdot 2\text{H}_2\text{O}$  (0.134 g, 0.5 mmol), 1,2'-Cy (0.085 g, 0.5 mmol), 4,4'-Bipy (0.078 g, 0.5 mmol) and 8 mL  $\text{H}_2\text{O}$  was stirred for 30 min, and then the pH value was adjusted to 7 with 1 M KOH. After stirring for another 30 min, the mixture was transferred to a 15 mL Teflon-lined stainless steel bomb and kept at 170°C under autogenously pressure for 5 days. The reaction system was cooled to room temperature during 24 h. A large amount of colorless block crystals of **II** were obtained. The yield was 55% based on Cd.

For  $\text{C}_{18}\text{H}_{16}\text{N}_2\text{O}_4\text{Cd}$

anal. calcd., %: C, 49.50; H, 3.69; N, 6.41.

Found, %: C, 49.42; H, 3.73; N, 6.38.

IR ( $\nu$ ,  $\text{cm}^{-1}$ ): 1539 s, 1480 s, 1390 s, 1218 w, 1067 m, 890 s, 812 s, 661 m, 615 s, 547 w, 491 s.

**Photocatalytic experiment.** The photocatalytic activities of the samples were evaluated by the degradation of RhB in the aqueous solution. 70 mL RhB aqueous solution with concentration of  $10^{-5}$  mol/L was mixed with 30 mg catalysts, which was exposed to illumination. Before turning on the lamp, the suspension containing RhB and photocatalyst were magnetically stirred in a dark condition for 40 min till an adsorption-desorption equilibrium was established. Samples were then taken out regularly from the reactor and centrifuged immediately for separation of any suspended solid. The transparent solution was analyzed by a UV-Vis spectrometer. An 11 W germicidal lamp ( $\lambda = 254$  nm) served as a UV light source. Langmuir-Hinshelwood (L-H) equation ( $r_0 = k_0 c_0 / 1 + K_0 c_0$ ) is employed to quantify the degradation reaction of RhB ( $r_0$  represents the initial rate,  $k_0$  represents the kinetic rate constant and  $K_0$  represents the adsorption coefficient of the reactant RhB). As the value of  $c_0$  is too small,  $K_0 c_0 \ll 1$ , the L-H rate expression can simply to first-order rate expression:  $r_0 = \text{d}C_0/\text{dt} = k_0 C_0$ . This

equation can be solved to obtain  $\ln(c/c_0) = -k_0 t$ . Based on Lambert-Beer law,  $c/c_0 = I/I_0$ , the equation can reduce to  $\ln(I/I_0) = -k_0 t$  finally.

**X-ray crystallography.** Suitable single crystals of **I** and **II** were carefully selected under an optical microscope and glued on glass fibers. Structural measurements were performed on a Bruker AXS SMART APEX II CCD diffractometer at 293 K. The structures were solved by the direct method and refined by the full-matrix least-squares method on  $F^2$  using the SHELXTL-97 crystallographic software package [26, 27]. Anisotropic thermal parameters were used to refine all non-hydrogen atoms. Carbon-bound hydrogen atoms were placed in geometrically calculated positions; oxygen-bound hydrogen atoms were located in the difference Fourier maps, kept in that position and refined with isotropic temperature factors. Further details of the X-ray structural analysis are given in Table 1. Selected bond lengths are listed in Table 2.

Supplementary material for complexes has been deposited with the Cambridge Crystallographic Data Centre (nos. 905357 (**I**) and 874125 (**II**); deposit@ccdc.cam.ac.uk or <http://www.ccdc.cam.ac.uk>).

## RESULTS AND DISCUSSION

Complex **I** exhibits an interesting 3D network. Cd(1) atom adopts distorted octahedron coordination mode and connects with three nitrogen atoms from three Bix ligands with Cd-N bond distances 2.273(4), 2.321(5), and 2.393(4) Å, respectively. The other coordination sites are occupied by three carboxylate oxygen atoms from two dcbpyno ligands with Cd-O bond distances range from 2.328(4) to 2.464(3) Å as shown in Fig. 1a. Two carboxylate groups in Dcbpyno ligands adopt two kind of connection mode, one is monodentate and the other is chelating. Further extension of the  $[\text{CdN}_3\text{O}_3]$  octahedron through the Dcbpyno ligands and bis-bridging Bix ligands results a 3D network, as shown in Fig. 2.

Complex **II** exhibits an interesting wavelike two-dimensional layer structure. There exists one crystallographically independent Cd atom in the fundamental unit as shown in Fig. 1b. Cd1 connects with four oxygen atoms from three 1,2'-Cy ligands with Cd-O bond distances range from 2.229(2) to 2.439(2) Å. Two nitrogen atoms from two 4,4'-Bipy ligands occupy the other two coordination sites. This results a distorted octahedron coordination mode of Cd(1). In complex **II**, one carboxylate group adopts chelating coordination mode, the other carboxylate group adopts bridging coordination mode. With this linking mode, adjacent Cd atoms are connected and form one-dimensional ladder-like structure along  $x$  axis. The 4,4'-Bipy ligands then connect neighboring

**Table 1.** Crystallographic data and experimental details for complexes **I** and **II**

Parameter	Value	
	<b>I</b>	<b>II</b>
Formula weight	780.06	436.73
Crystal system	Monoclinic	Triclinic
Space group	<i>C</i> 2/c	<i>P</i> 1
Unit cell dimensions:		
<i>a</i> , Å	25.469(2)	7.7499(16)
<i>b</i> , Å	15.3912(12)	9.5902(19)
<i>c</i> , Å	17.1439(13)	11.860(2)
α, deg		113.30(3)
β, deg	98.7910(10)	99.40(3)
γ, deg		93.88(3)
<i>V</i> , Å <sup>3</sup>	6641.4(9)	790.1(3)
<i>Z</i>	8	2
ρ <sub>calcd</sub> , g/cm <sup>3</sup>	1.560	1.836
μ, mm <sup>-1</sup>	0.722	1.409
<i>F</i> (000)	3176	436
θ Range, deg	1.55–25.00	3.30–25.00
Reflections collected	19379	6215
<i>R</i> <sub>int</sub>	0.0312	0.0227
Reflections with <i>I</i> > 2σ( <i>I</i> )	5851	2762
Max, min transmission	0.891, 0.859	0.765, 0.700
Goodness-of-fit on <i>F</i> <sup>2</sup>	1.113	1.050
Data/restraints/parameters	5851/6/453	2762/0/234
Final <i>R</i> indices ( <i>I</i> > 2σ( <i>I</i> ))*	<i>R</i> <sub>1</sub> = 0.0504, <i>wR</i> <sub>2</sub> = 0.1700	<i>R</i> <sub>1</sub> = 0.0233, <i>wR</i> <sub>2</sub> = 0.0731
<i>R</i> indices (all data)	<i>R</i> <sub>1</sub> = 0.0623, <i>wR</i> <sub>2</sub> = 0.1871	<i>R</i> <sub>1</sub> = 0.0257, <i>wR</i> <sub>2</sub> = 0.0823
Largest diff. peak and hole, <i>e</i> /Å <sup>3</sup>	0.508 and –0.528	0.560 and –0.793

\* *R*<sub>1</sub> = Σ|*F*<sub>o</sub>| – |*F*<sub>c</sub>|/Σ|*F*<sub>o</sub>|; *wR*<sub>2</sub> = Σ[w(*F*<sub>o</sub><sup>2</sup> – *F*<sub>c</sub><sup>2</sup>)<sup>2</sup>/Σw(*F*<sub>o</sub><sup>2</sup>)<sup>2</sup>]<sup>1/2</sup>.

**Table 2.** Bond lengths (Å) for complexes **I** and **II**\*

Bond	<i>d</i> , Å	Bond	<i>d</i> , Å
<b>I</b>			
Cd(1)–O(1)	2.464(3)	Cd(1)–O(2)	2.457(4)
Cd(1)–O(4) <sup>#1</sup>	2.328(4)	Cd(1)–N(3)	2.273(4)
Cd(1)–N(5) <sup>#2</sup>	2.393(4)	Cd(1)–N(7)	2.321(5)
<b>II</b>			
Cd(1)–O(1)	2.439(2)	Cd(1)–O(2)	2.313(2)
Cd(1)–O(3) <sup>#1</sup>	2.229(2)	Cd(1)–O(4) <sup>#2</sup>	2.234(2)
Cd(1)–N(1)	2.380(3)	Cd(1)–N(2) <sup>#3</sup>	2.362(3)

\* Symmetry transformations used to generate equivalent atoms:

<sup>#1</sup> –*x* + 3/2, *y* – 1/2, –*z* + 3/2; <sup>#2</sup> *x*, –*y* – 1, *z* – 1/2 (**I**); <sup>#1</sup> –*x* + 2, –*y* + 2, –*z* + 1; <sup>#2</sup> *x* – 1, *y*, *z*; <sup>#3</sup> *x*, *y*, *z* + 1 (**II**).

chains together and form an interesting wavelike two-dimensional layer structure of complex **II** (Fig. 3).

In order to examine the thermal stabilities of complex **I**, TGA was carried out. Complex exhibits one-step weight loss. The weight loss about 74.43% occurs in the range of 312 to 487°C, corresponding to the loss of organic ligands (calcd. 74.19%).

Photocatalytic activity property studies were investigated by the degradation of RhB. In visible light region, pure complex **I** displays no effect on RhB because it can not be excited by visible light. When excited by UV light, complex **I** exhibits photocatalytic activity, in 300 min, about 71% RhB decompose and the rate constant is 0.00514 min<sup>-1</sup> (Fig. 4). For photocatalytic degradation reaction, the activity of recycled catalyst is a very important factor to determine the performance of a photocatalyst. Here, the photocata-

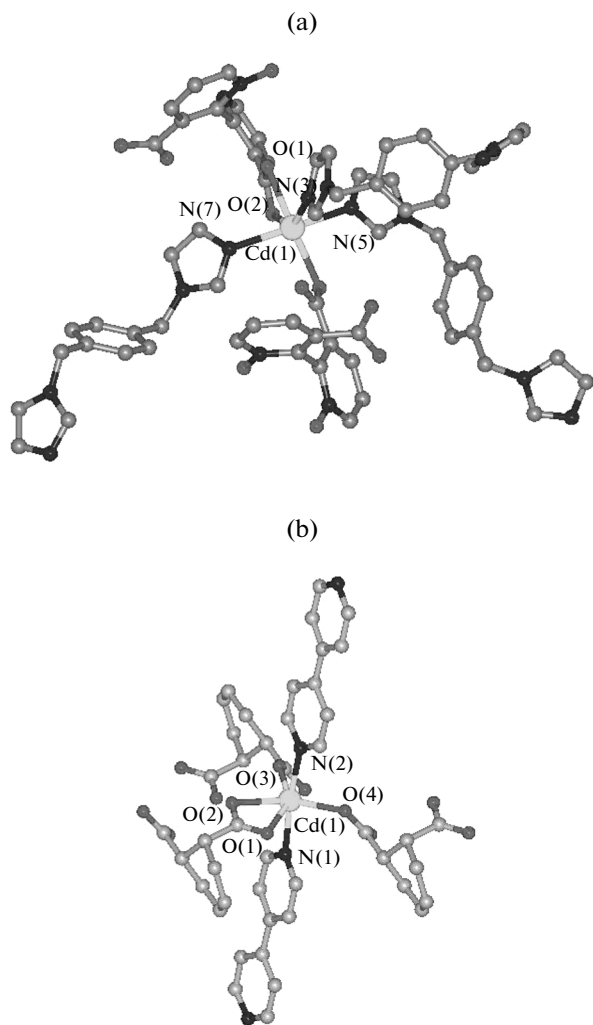


**Fig. 1.** The fundamental units of complexes **I** (a) and **II** (b).

lytic reaction is re-examined for five times (Fig. 5). The recycled complex **I** still exhibits excellent catalytic property and the relationship of degradation rate and time is very similar between every cycle, which indicates its high stability during the decomposition process of organic dyes. Based on the experimental findings and observations, we speculate the mechanism as follows. For complex **I**, under the irradiation of UV light, the electrons are excited from the valence band and transferred to the conduction band, simultaneously, positive charged holes are formed in valence band. After migrate to the surface of complex **I**, the electrons reduce the oxygen ( $O_2$ ) to super oxide radical ( $O_2^-$ ) and holes oxidize the hydroxyl ( $H_2O$ ) to hydroxyl radicals ( $\cdot OH$ ). These oxygen radicals and hydroxyl radicals are responsible for the degradation of RhB.

The fluorescent spectrum of complex **II** is shown in Fig. 6. It can be observed that this complex exhibit

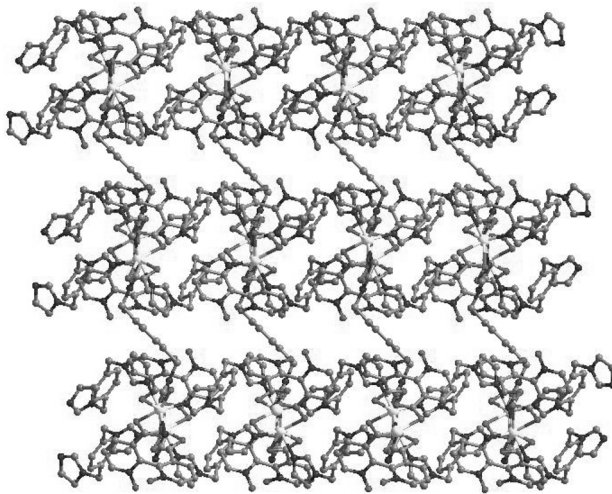


**Fig. 2.** The two-dimensional wavelike layer structure of complex **I**.

photoluminescence with emission maximum at ca. 425 nm upon excitation at 340 nm. According to the previous reports, these emission bands could be assigned to the emission of ligand-to-metal charge transfer (LMCT) [28].

In this article, we successfully combined the merits of Dcbpyno, 1,2'-Cy and nitrogen containing ligands with Cd salt and synthesized two interesting coordina-

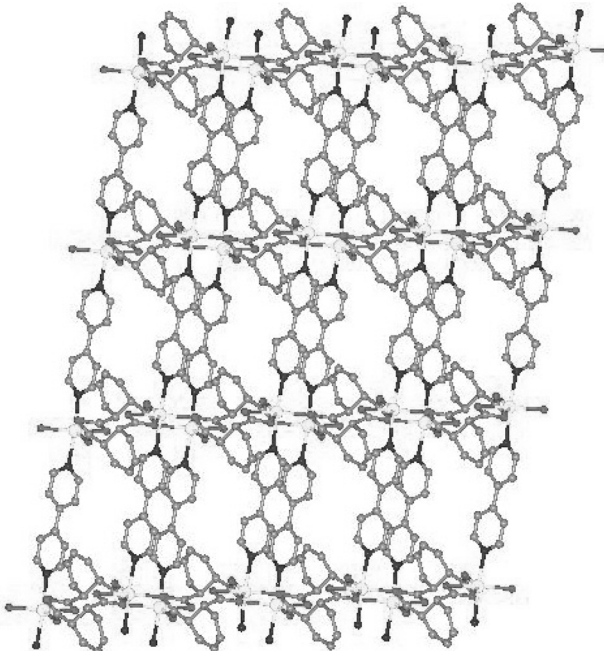


**Fig. 3.** The three-dimensional network of complex **II**.

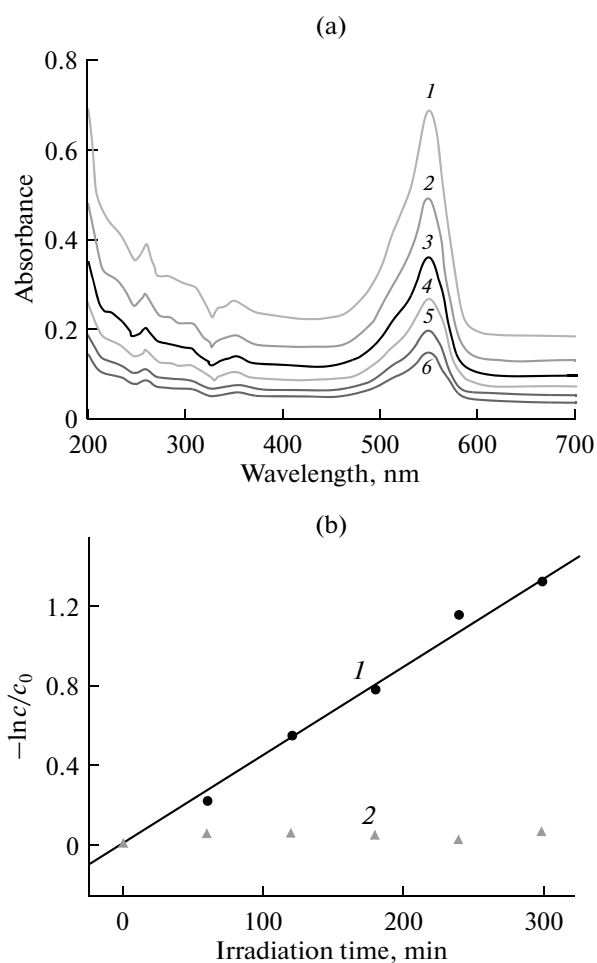


**Fig. 4.** (a) UV-Vis absorption spectra of RhB solution degraded by complex I under UV light: 0 (1), 60 (2), 120 (3), 180 (4), 240 (5), 300 min (6); (b) curve of degradation rate for RhB by complex I under different conditions as the function of irradiation time: UV (1) and visible (2) light.

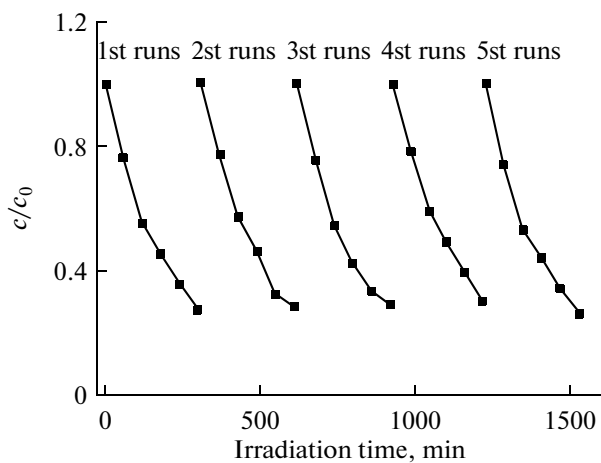


**Fig. 5.** Cycling runs of the photocatalytic degradation of RhB in the presence of complex I.

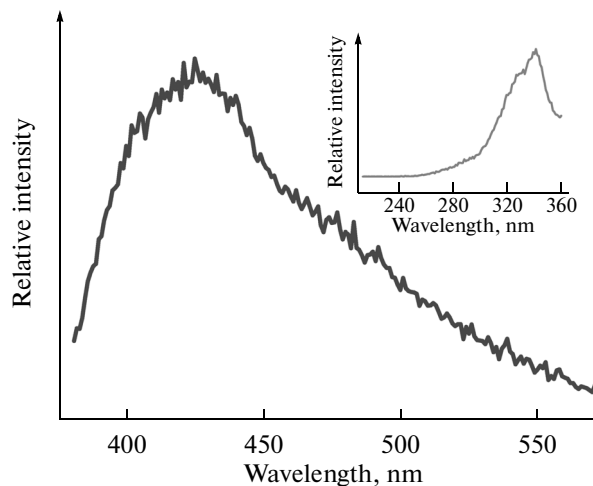


**Fig. 6.** The fluorescent spectrum of complex II.

tion polymers. Furthermore, the photocatalytic property of complex I and the fluorescent property of complex II were reported.

## REFERENCES

1. Batten, S.R. and Robson, R., *Angew. Chem. Int. Ed.*, 1998, vol. 37, p. 1460.
2. Carlucci, L., Ciani, G., and Proserpio, D.M., *Coord. Chem. Rev.*, 2003, vol. 246, p. 247.
3. Xu, S.P. and Pei, Y., *J. Chem. Crystallogr.*, 2012, vol. 42, p. 330.
4. Xu, W. and Zheng, Y.Q., *J. Chem. Crystallogr.*, 2012, vol. 42, p. 313.
5. Zhang, Z.Y., *J. Chem. Crystallogr.*, 2012, vol. 42, p. 333.
6. Xu, X.X., Liu, X.X., Sun, T., et al., *J. Coord. Chem.*, 2009, vol. 62, p. 2755.
7. Xu, X.X., Lu, Y., Wang, E.B., et al., *Cryst. Growth Des.*, 2006, vol. 6, p. 2026.
8. Yang, Q.Y., Zhang, S.R., Yang, R., et al., *CrystEngComm*, 2009, vol. 11, p. 680.
9. Guo, H.D., Qiu, D.F., Guo, X.M., et al., *CrystEngComm*, 2009, vol. 11, p. 2611.
10. Guo, L., Wu, G., and Li, H.H., *J. Chem. Crystallogr.*, 2012, vol. 42, p. 192.
11. Jin, S.W. and Wang, D.Q., *J. Chem. Crystallogr.*, 2012, vol. 42, p. 276.
12. Sun, H.L., Wang, Z.M., Gao, S., and Batten, S.R., *CrystEngComm*, 2008, vol. 10, p. 1796.
13. Du, J.L., Hu, T.L., Zhang, S.M., et al., *CrystEngComm*, 2008, vol. 10, p. 1866.
14. Wang, X.L., Bi, Y.F., Chen, B.K., et al., *Inorg. Chem.*, 2008, vol. 47, p. 2442.
15. Wang, R.H., Yuan, D.Q., Jiang, F.L., et al., *Cryst. Growth Des.*, 2006, vol. 6, p. 1351.
16. Wang, R.H., Han, L., Jiang, F.L., et al., *Cryst. Growth Des.*, 2005, vol. 5, p. 129.
17. Wang, R.H., Zhou, Y.F., Sun, Y.Q., et al., *Cryst. Growth Des.*, 2005, vol. 5, p. 251.

18. Wang, R.H., Yuan, D.Q., Jiang, F.L., et al., *Cryst. Growth Des.*, 2006, vol. 6, p. 1351.
19. Liu, J.Q., Wang, Y.Y., and Huang, Y.S., *CrystEngComm*, 2011, vol. 13, p. 3733.
20. Tao, J., Tong, M.L., and Zhang, X.M., *Dalton Trans.*, 2001, p. 770.
21. Xu, X.X., Liu, X.X., Sang, X.G., et al., *J. Chem. Cryst. Logogr.*, 2011, vol. 41, p. 453.
22. Xu, X.X., Zhang, X., Liu, X.X., et al., *Cryst. Growth Des.*, 2010, vol. 10, p. 2272.
23. Xu, X.X., Lu, Y., Wang, E.B., et al., *Inorg. Chim. Acta*, 2007, vol. 360, p. 455.
24. Xu, X.X., Ma, Y., and Wang, E.B., *J. Solid State Chem.*, 2007, vol. 180, p. 3136.
25. Thirumurugan, A., Avinash, M.B., and Rao, C.N.R., *Dalton Trans.*, 2006, p. 221.
26. Sheldrick, G.M., *SHELXTL-97, Program for Crystal Structure Refinement*, Göttingen (Germany): Univ. of Göttingen, 1997.
27. Sheldrick, G.M., *SHELXTL-97, Program for Crystal Structure Solution*, Göttingen (Germany): Univ. of Göttingen, 1997.
28. Zheng, S.L. and Cheng, X.M., *Aust. J. Chem.*, 2004, vol. 57, p. 703.